ELSEVIER

Biochimica et Biophysica Acta 1413 (1999) 43–49

BIOCHIMICA ET BIOPHYSICA ACTA
BBA

www.elsevier.com/locate/bba

Relative positions of electron transfer components in Photosystem II studied by '2+1' pulsed electron paramagnetic resonance: Y_D and Q_A

Takahiko Yoshii [a], Asako Kawamori [a,*], Motoyoshi Tonaka [a], Kozo Akabori [b]

[a] *Faculty of Science, Kwansei Gakuin University, Nishinomiya 662-8501, Japan*
[b] *Faculty of Integrated Arts and Sciences, Hiroshima University, Higashi-Hiroshima 739-8521, Japan*

Received 19 May 1999; received in revised form 14 July 1999; accepted 22 July 1999

Abstract

A '2+1' electron spin echo (ESE) method, to measure the dipole interaction between paramagnetic centers directly, has been applied to determine the orientation of the radius-vector $\mathbf{R}_{D-Q}$ (Y_D to Q_A) in a membrane oriented Fe^{2+}-depleted preparation of Photosystem II. Using the distance of $\mathbf{R}_{D-Q} = 38.5 \pm 0.8$ Å determined for the non-oriented membranes, the angle between $\mathbf{R}_{D-Q}$ and the membrane normal $\mathbf{n}$ was determined to be $\theta_0 = 13.0 \pm 4.0°$. The distance and angle of another related pair of radicals, $\mathbf{R}_{P680-D}$, were suggested to be 20 Å and 42°, respectively, based on the above data and ESEEM of the $P680^+Q_A^-$ in the oriented membranes.

Keywords: Photosystem II; Structural organization; Y_D; Q_A; Electron spin echo, '2+1'; Oriented membrane

1. Introduction

In higher plant Photosystem II (PS II) that oxidizes water and reduces quinones is a membrane protein complex composed of several intrinsic and extrinsic polypeptides. Two 32-kDa polypeptides are called D1 protein containing Q_B (quinone B) and Y_Z (tyrosine Z), and D2 protein containing Q_A (quinone A) and Y_D (tyrosine D). The reaction center P680 (pigment 680 nm) in PS II is thought to be a chlorophyll *a* dimer situated at the symmetry center of both proteins [1–3].

Only one component, the tyrosine radical Y_D^+, is usually observable at 273 K in the dark by electron paramagnetic resonance (EPR) [2]. Y_D^+ has been known to give an EPR signal at $g = 2.0046$ with about 2 mT width. Though Y_D does not directly participate in the reactions related to the normal electron transfer process and its role in PS II is rather unclear, a variety of works have been carried out on the EPR of Y_D^+ as a monitor for the structure and functions of PS II [1–3].

The primary electron acceptor quinone, Q_A, is a plastoquinone-9, normally participating in one electron redox chemistry involving a semiquinone state. The electron on Q_A^- is transferred to another plasto-

Abbreviations: PS II, Photosytem II; Y_D, tyrosine-161 in D2 subunit of plant PS II; P680, the primary electron donor in PS II; Q_A, the primary electron acceptor in PS II; Q_B, the secondary electron acceptor in PS II; Y_Z, Tyrosine-161 in D1 subunit of PS II; EPR, electron paramagnetic resonance; ESE, electron spin echo; ELDOR, electron–electron double resonance; ESEEM, electron spin echo envelope modulation; m.w., microwave; cw, continuous wave; PMSF, phenylmethylsulfonylfluoride; MES, 2-morpholinoethanesulfonic acid; Tris, Tris(hydroxymethyl)aminomethane

* Corresponding author. Fax: +81-798-51-0914.

0005-2728/99/$ – see front matter
PII: S0005-2728(99)00082-1

quinone, Q_B, which, by contrast, exists under physiological conditions not only in semiquinone, but also in a quinol form.

In ordinary untreated or Tris-treated PS II membranes [4], the magnetic interaction of the reduced Q_A^- with the nearby non-heme Fe^{2+} leads to a 40 mT width EPR spectrum. This $Fe^{2+}Q_A^-$ signal can be observed only under temperatures below 8 K at field positions of $g = 1.65$, 1.82, and 1.95, depending on pH [1,4]. However, there are several methods to decouple the magnetic interaction of Q_A^- from the non-heme iron: (1) removal of the non-heme Fe^{2+} [5,6]; (2) substitution by diamagnetic Zn^{2+} as described in [7]; (3) cyanide treatment to convert the high spin ($S = 2$) to low spin ($S = 0$) of the non-heme Fe^{2+} [8]; (4) high pH (about 11) treatment [9]. With one of these means, a sharp Q_A^- EPR signal (at $g = 2.0045$ with a 0.9 mT width), magnetically decoupled from the non-heme Fe^{2+}, can be observed.

In this work, we used PS II preparations depleted of the non-heme Fe^{2+} to eliminate the strong magnetic interaction, because iron-depleted samples retained the native function and structure more than the cyanide-treated PS II membrane fragments [10].

For PS II of oxygenic photosynthesis, a detailed structural model based on X-ray or electron crystallography has not yet become available and the positions of electron transfer components are unknown. ESEEM of spin polarized radical [11,12] and the '2+1' electron spin echo (ESE) method (a special case of general electron–electron double resonance (ELDOR) methods) were applied to measure directly the dipole interaction between the radical centers [13,14]. By using these methods, it has been possible to improve the accuracy in determining distances between the redox-active components in PS II [15–19]. Furthermore, it is highly desirable to clarify a three-dimensional arrangement of electron transfer components using the oriented PS II particles. There are several works about the orientated PS II membranes used to elucidate the molecular orientation of the electron carrier under investigation with respect to the membrane plane [20–24].

In this work, we have used the oriented membranes to obtain the angular information for Y_D–Q_A distance vector $\mathbf{R}_{D-Q}$ in Fe^{2+}-depleted preparation of PS II by using the '2+1' pulse sequence ESE method.

2. Materials and methods

The PS II membranes were prepared from spinach by the method of Kuwabara and Murata [25]. The PS II core complexes were prepared by removing the light-harvesting proteins from the PS II particles, as described in [26]. Tris-treatment was performed by incubation of the core complexes on ice in a buffer; 0.8 M Tris-HCl (pH 8.8), 10 mM Na_2-EDTA, for 30 min under room light [4].

Removal of non-heme Fe^{2+} from the core complex was carried out by a slightly modified procedure of Klimov et al. [5] in the presence of a serine type proteinase inhibitor (PMSF, 100 μM) in all the process of preparation. These core complexes were suspended in a buffer solution of 0.4 M sucrose, 10 mM NaCl, 50 mM MES (pH 6.0). After centrifugation at $35\,000 \times g$, the pellets were suspended in the above buffer solution with 70% glycerol added and stored in liquid nitrogen until use. All treatments were performed at about 4°C under a dim green light.

For measurements of oriented PS II particles, after elimination of glycerol, the membranes were dried on pieces of mylar sheets at 0°C for about 16 h using nitrogen gas flow under controlled humidity of 90% [20]. Five mylar sheets with 3×20 mm^2 with each dried sample were put into an EPR tube of an inner diameter of 4 mm.

Before EPR experiments, the sample was illuminated by a 500-W tungsten-halogen lamp through a 10-cm-thick water filter at 273 K for 5 min, followed by dark-adaptation for 3 min at 273 K to make Chlz^+ radicals decay [27]. Then the sample was frozen quickly in liquid nitrogen to trap $Y_D^+Q_A^-$ radicals.

To check the trapped radicals, cw-EPR experiments have been performed on a Varian E-109 X-band EPR spectrometer equipped with a TE_{102} rectangular cavity by using a finger-type dewar at 77 K.

The '2+1' ESE experiments have been performed on a Bruker ESP-380 X-band pulsed EPR spectrometer equipped with a Bruker ER4117 DHQ-H cylindrical dielectric cavity and a nitrogen gas flow system (CF935, Oxford Instruments). The field sweep ESE was obtained with a boxcar gate averager and a signal processor (EG&G Princeton Applied Research, Model 4420 and 4402). The measurement temperature was about 80 K and microwave pulses of 16, 24 and 16 ns duration were applied. The m.w. magnetic

field amplitude, H_1, in the three pulses was set to provide the spin rotation angles of 30°, 60° and 30°, respectively, in the pulse sequence shown in Fig. 1.

3. Theory

The principles of '2+1' ESE method have been described in detail [13,14,28,29] and in our previous works on PS II [15,17–19]. In '2+1' ESE method, the pulse sequence was applied as shown in Fig. 1.

A primary ESE signal is formed by the first and third m.w. pulses separated by the time interval τ. When the second pulse with varying time interval τ' is applied, the ESE amplitude oscillates with a frequency proportional to the value of magnetic dipole interaction at a given orientation. The oscillation amplitude of this signal is given as a function of the second pulse, τ' [15].

$$V(\tau,\ \tau') \propto 1-2\langle S_3\rangle \sin^2(\pi D\tau)-2\langle S_2\rangle \sin^2(\pi D\tau')+ \langle S_2S_3\rangle\,[\sin^2(\pi D\tau')-\sin^2(\pi D(\tau'-\tau))+\sin^2(\pi D\tau)] \quad (1)$$

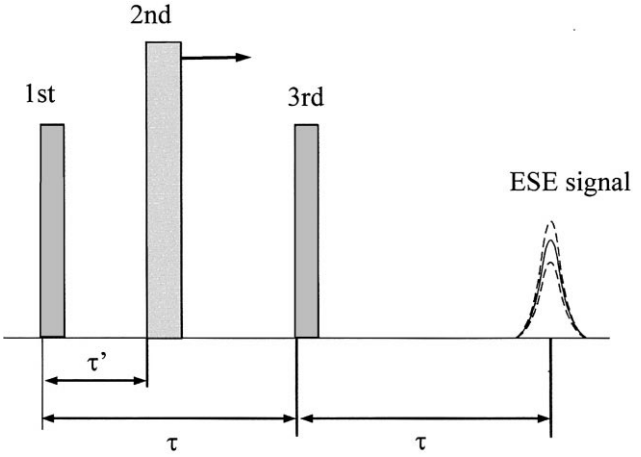

Fig. 1. The pulse sequence for a '2+1' ESE method. The primary ESE signal is formed by the first and third m.w. pulses with a carrier frequency ω, separated by the time interval τ. The amplitude of the ESE signal is observed as a function of the position τ' of the second m.w. pulse with the same carrier frequency ω as shown in Eq. 1. The m.w. field amplitude, H_1, in three pulses was set to provide the spin rotation angles 30°, 60° and 30°, respectively.

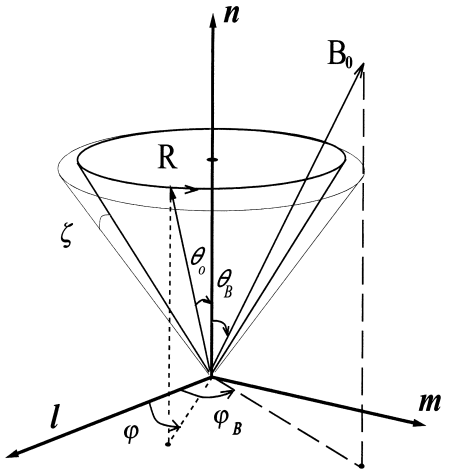

Fig. 2. Orientation of membranes and the magnetic field $\mathbf{H}_0$ with respect to the membrane coordinate system (***l***, ***m***, ***n***), where ***n***-axis is the membrane normal while ***l*** and ***m*** are arbitrarily selected orthogonal axes in the membrane plane. All orientations obtained by rotation of PS II around ***n*** by an arbitrary angle φ are assumed to have equal probability. Deviation of the ***n***-axis from an average orientation is taken into consideration as a Gaussian distribution function of ζ which is converted to the deviation of the magnetic field direction θ–θ_B. See text for details.

and

$$D = D_0\,(1-3\cos^2\theta_R) \quad (2)$$

where, D is the secular component of the dipole interaction between the radical spins with θ_R being the angle between the static magnetic field $\mathbf{B}_0$ and the radius-vector $\mathbf{R}$ joining the spins in the pair, S_2 and S_3 characterize the excitation of spins by the second and third m.w. pulses, respectively. The dipole interaction constant D_0 is derived by fitting Eq. 1 to the observed '2+1' ESE, from which the distance between the spins can be calculated using a point-dipole approximation as given;

$$D_0 = (g\beta)^2/hR^3 \quad (3)$$

The calculation of the angle θ_R between $\mathbf{R}_{D-Q}$ for $Y_D^+Q_A^-$, and the membrane normal $\mathbf{n}$ is given by [19].

$$\cos\theta_R = \cos\theta_0\cos\theta_B + \sin\theta_0\sin\theta_B\cos(\phi_B-\phi) \quad (4)$$

here, θ_B is the angle between $\mathbf{B}_0$ and $\mathbf{n}$, ϕ_B is the angle describing a rotation of $\mathbf{B}_0$ around the $\mathbf{n}$-axis as shown in Fig. 2. In an oriented system, Eq. 1 is to

be averaged over the angles ϕ, and ϕ_B;

$$\langle V(\tau,\ \tau')\rangle_{\text{ori.}} \propto \int_0^{2\pi}\int_0^{2\pi} V\ (\tau,\ \tau')\ d\phi_B d\phi \qquad (5)$$

Actually, the deviation from the average orientation of the membrane normal should be taken into consideration as a Gaussian distribution $G(\theta-\theta_B)$.

$$\langle V(\tau,\ \tau')\rangle_{\text{ori.}} \propto \int_0^{\pi}\int_0^{2\pi}\int_0^{2\pi} V(\tau,\ \tau')$$

$$d\phi_B d\phi\, G\ (\theta-\theta_B)\sin\theta d\theta \qquad (6)$$

where $G(\theta-\theta_B) = N\exp(-\zeta^2/\zeta_0^2)$ with $\zeta = \theta-\theta_B$ and ζ_0 is a root mean square deviation and N is a normalization factor.

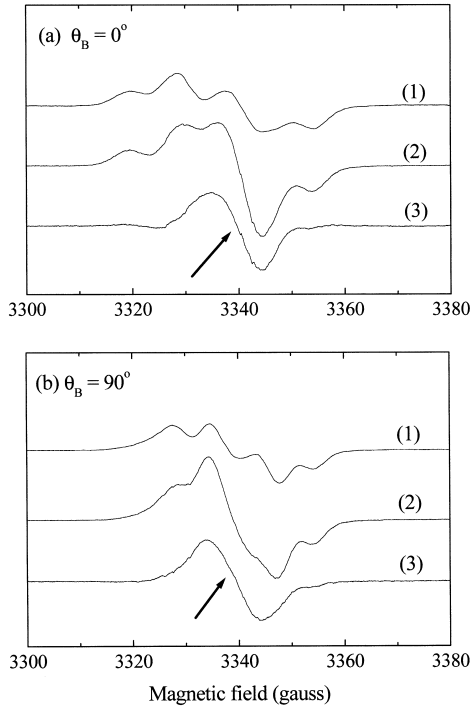

Fig. 3. The cw EPR spectra in Fe^{2+}-depleted PS II at the angles θ_B of 0° (a) and 90° (b), respectively. Y_D^+ and Q_A^- radicals were trapped by illumination at 273 K for 5 min followed by dark-adaptation at 273 K for 3 min. Traces 1 and 2 show the signals of dark-adapted (Y_D^+ only before illumination) and illuminated (Y_D^+ and Q_A^-) samples, respectively. Traces 3 show subtracted spectra (2)−(1) corresponding to Q_A^- spectra. The arrow shows the spectral position $g = 2.0045$ (the center of Q_A^- signal), where the '2+1' ESE was measured. Experimental conditions of cw-EPR: temperature, 77 K; microwave frequency, 9.34 GHz; microwave power, 0.25 μW; field modulation frequency, 100 kHz; field modulation amplitude, 3.2 Gauss.

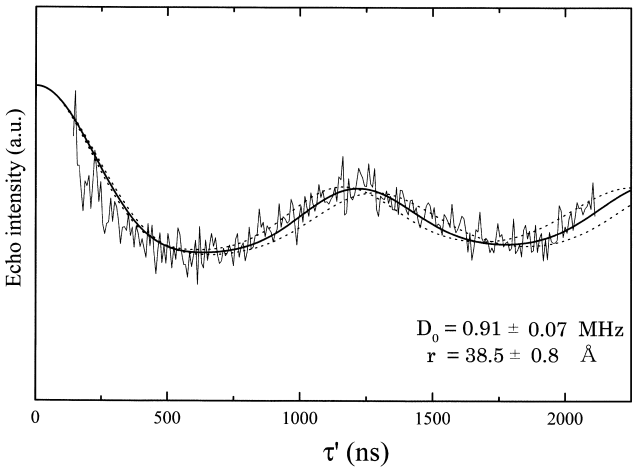

Fig. 4. The '2+1' ESE trace of Y_D^+ and Q_A^- radical pair in a non-oriented sample observed at 80 K. Solid line, calculated for the dipole interaction constant $D_0 = 0.91$ MHz ($D_0 = (g\beta)^2/hr^3$). From this value, the distance between Y_D^+ and Q_A^- is derived to be 38.5 ± 0.8 Å. Dashed lines, calculated for frequencies of error limits of ±0.7 MHz. Experimental conditions: temperature, 80 K; $\tau = 2000$ ns; the magnetic field, 3460 Gauss; m.w. frequency, 9.61 GHz.

4. Results

Fig. 3 shows the cw-EPR spectra in Fe^{2+}-depleted PS II observed at the angles θ_B of 0° (a) and 90° (b), respectively. Traces 1 and 2 show the spectra of dark-adapted (Y_D^+ only) and illuminated (Y_D^+ and Q_A^-) PS II particles, respectively. Traces 3 in Fig. 3a and b show the difference spectra of illuminated and dark adapted PS II samples. EPR spectra for oxidized tyrosines Y_D^+ and reduced Q_A^- overlapped in the sample trapped in liquid nitrogen, after illumination for 5 min followed by dark adaptation for 3 min. The trapped tyrosine can be assigned to Y_D^+ only (not Y_Z^+) as reported by [18]. Trace 1 for the dark-adapted sample indicates the signal of Y_D^+ only. Traces 2 give the trapped Q_A^- EPR signal at the angles θ_B of 0° and 90°, respectively, by subtraction of trace 1 as shown in traces 3. Obtained structureless Q_A^- EPR signals have about 0.9 mT widths at $g = 2.0045$. The yield of Q_A^- in Trace 3 estimated by division with double integration of the spectra in Trace 1 was about 60% of that of Y_D^+. The Q_A^- signals showed only a slight anisotropy, while Y_D^+ signal did typical line shapes depending on orientation [20].

In Fig. 4, the '2+1' ESE trace of Y_D^+ and Q_A^- radical pair in non-oriented sample observed at 80 K is

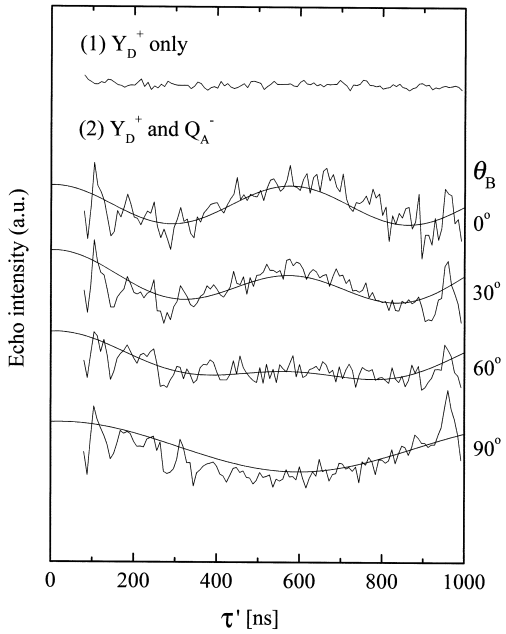

Fig. 5. The '2+1' ESE traces recorded in the Fe^{2+}-depleted membranes for the orientations with $\theta_B = 0°$, 30°, 60° and 90°, respectively. Trace 1 shows the time profile observed in the dark-adapted (Y_D^+ only) for $\theta_B = 0°$ and traces 2 show the profiles in the illuminated (Y_D^+ and Q_A^-) samples, for 0°, 30°, 60°, and 90°, respectively. Experimental conditions: the same as in Fig. 4 except for $\tau = 1080$ ns. Solid lines show calculated values based on Eq. 5 for $D_0 = 0.91$ MHz in Fig. 4, and the angle $\theta_0 = 13.0°$, between $\mathbf{R}_{D-Q}$ and the **n**-axis. Deviation of the membrane normal from the average orientation is taken into consideration as a Gaussian distribution function of ζ ($= \theta - \theta_B$) with the value of $\zeta_0 = 15°$. See text for details.

shown. In this experiment, a fixed $\tau = 2000$ ns, with τ' varying from 40 to 1960 ns, was applied, where the magnetic field was fixed at the center of the overlapped signal ($g = 2.0045$) as indicated by the arrows in Fig. 3. This ESE signal shows an oscillation due to the dipole interaction between Y_D^+ and Q_A^-. To determine the value of the dipole interaction constant D_0, simulations were carried out to fit the experimental time profile as in [15]. These calculations allowed one to determine the value of dipole interaction $D_0 = 0.91 \pm 0.07$ MHz. From this value, the distance between Y_D^+ and Q_A^- is estimated $r = 38.5 \pm 0.8$ Å. The distance of 38.5 Å in Fe^{2+}-depleted PS II was almost same as that in a cyanide-treated PS II sample [18].

Trace 1 in Fig. 5 was recorded for dark-adapted Fe^{2+}-depleted PS II particles with the orientation $\theta_B = 0°$ that shows Y_D^+ signal only. For other orientations the similar time profiles were obtained. In this experiment, a fixed $\tau = 1080$ ns, with τ' varying from 40 to 960 ns was applied, where the magnetic field was fixed at the center of signal as indicated by the arrow in Fig. 3.

The '2+1' ESE traces were recorded for the illuminated Fe^{2+}-depleted PS II particles at the orientations with $\theta_B = 0$, 30, 60 and 90°, respectively, in trace 2 of Fig. 5. The τ' dependence reveals about one period of low frequency oscillation for $\theta_B = 90°$, especially, and differs remarkably from that obtained in the dark-adapted sample. Therefore, in the illuminated sample, there exists the dipole interaction between Y_D^+ and Q_A^-. The spectrum of illuminated sample for $\theta_B = 0°$ has an approximate twice the oscillation frequency of that for $\theta_B = 90°$. The fast oscillation component of about 70 ns period is ascribed to matrix proton ESEEM as in [19].

Using $D_0 = 0.91$ MHz found for the Y_D^+ and Q_A^- pair, the value of the dipole interaction in Fig. 4, we determine the angle between the radius vector from Y_D to Q_A, $\mathbf{R}_{D-Q}$, and the membrane normal, **n**. For the deviation of orientation from the average normal, a Gaussian distribution function of ζ ($= \theta - \theta_B$) as given by $(1/\sqrt{2\pi}\langle\zeta_0^2\rangle)\exp[(1/2)\ \zeta^2/\langle\zeta_0^2\rangle]$ is taken into consideration, where $\langle\zeta_0^2\rangle$ is a mean square deviation. Taking $\zeta_0 = 15°$, simulations were carried out applying Eqs. 1–4 to fit the oscillation pattern. Successful fits with the oscillation time profile observed by '2+1' sequence for $\theta_B = 0$–90° were obtained.

In Fig. 5, the straight lines show the simulation values for orientations $\theta_B = 0$–90°, respectively. The angular dependence of '2+1' ESE spectra suggests that the angle between $\mathbf{R}_{D-Q}$, and the **n**-axis is $13.0 \pm 4°$.

5. Discussion

The distance between Y_D and Q_A radical pair was estimated to be 38.5 ± 0.8 Å in this work, which is consistent with that in our previous work for cyanide-treated PS II [18]. The angular dependence of '2+1' ESE spectra in this work suggests that the angle between $\mathbf{R}_{D-Q}$, and the **n**-axis was to be $13.0 \pm 4.0°$. In the recent works [30,31], an electron crystallography method was applied to analysis of

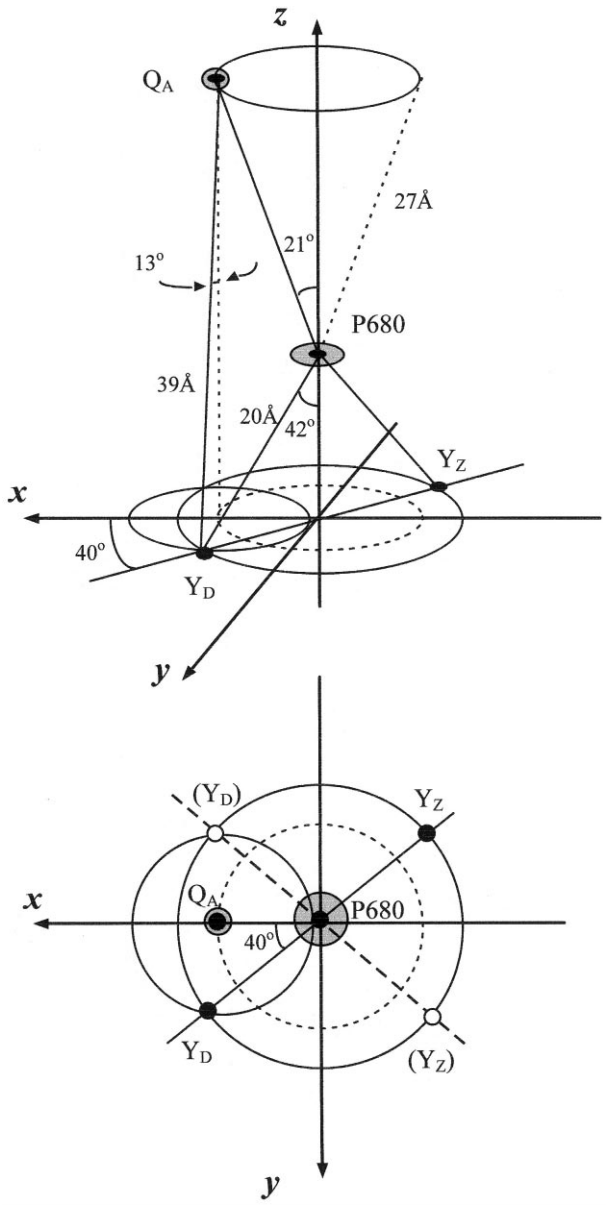

Fig. 6. The relative positions of electron transfer components Y_D, Y_Z, P680 and Q_A. Y_D and Y_Z are thought to be located in *C2* symmetry with respect to P680. The distance between P680 and Y_D or Y_Z is about 20 Å. Their orientations are about $\tan^{-1}$ (13/14.5) = 42° from the membrane normal **n**. The direction cosine of the vector $\mathbf{R}_{P680-D}$ from Y_D to P680 on the membrane plane is about 40° from that of $\mathbf{R}_{P680-Q}$. The circled dark areas show the ranges for ambiguity of positions of P680 and Q_A, respectively.

the three-dimensional structure of the plant PS II. However, the resolution of 8 Å was not enough to determine the positions of electron transfer components except for chlorophyll molecules. The structural analyses of PS II by pulsed EPR have given important information to investigate the function and structure relation of PS II in the present situation of the lack of direct X-ray structure data.

In the previous works [32], the redox properties of PS II and bacterial reaction centers are similar on the acceptor side. Furthermore, there has been suggested also a structural similarity in the primary sequences of PS II and purple bacterial reaction center proteins [33,34]. However, they are quite different on the donor side. In purple bacteria, the oxidized donor is reduced by a cytochrome. On the contrary, in the PS II the secondary donor is a tyrosine located at 161 in D1 protein. Accordingly, the bacterial reaction center structure will not be applied to deduce the angle between $\mathbf{R}_{D-Q}$ and the **n**-axis.

In our previous works, several distances were determined in pairs of paramagnetic components of PS II, Y_D–Mn cluster, Y_Z–Y_D, Y_D–Q_A Y_D–Chl_Z by pulsed ELDOR and '2+1' pulse sequence [17,18] and P680–Q_A by spin-polarized ESEEM [11]. These distances are accurate enough within 1 Å error. The angles of distance vector relative to the membrane normal were determined within 2° uncertainty [19]. The distance from Y_Z or Y_D to another electron transfer component on the donor side may be derived using these data.

Recently, the angle between $\mathbf{R}_{P680-Q}$ for $P680^+Q_A^-$ radical pair and the **n**-axis has been determined to be 21° [35] in addition to the distance of 27 Å [11]. Combining with the result obtained in this work and the distance of 29 Å determined [15,17] between Y_D^+ and Y_Z^+ radical pairs, the distance between P680 and Y_D or Y_Z can be derived by a geometrical drawing. In Fig. 6, a three-dimensional arrangement of electron transfer components Y_D, Y_Z, P680 and Q_A are derived using the assumption that Y_D and Y_Z are thought to be located in *C2* symmetry with respect to P680. Actually, the direction from Y_D to Y_Z is inclined by about 10° from the membrane plane [19], which may be neglected as the first approximation. Using these values of distances and angles, the distances of Y_D– and Y_Z–P680 are calculated to be about 20 Å, respectively. The angles of $\mathbf{R}_{P680-D}$ for P680–Y_D or $\mathbf{R}_{P680-Z}$ for P680–Y_Z is estimated to be about 42° from the membrane normal **n**. In this work combined with the results of our previous works [15,35], new structural information about P680 and

the secondary donors have been derived. However, we have to notice some limitation of distance and angle determination, because we used an assumption of point dipole on each radical. Actually, the spin density is delocalized especially on the $P680^+$ dimer with the one dimer half dominantly occupied [36]. Therefore, the above-derived values are considered to be tentative ones. Further refinement for the distance and angle for $\mathbf{R}_{P680-D}$ or $\mathbf{R}_{P680-Z}$ will be expected when the correct molecular shape and spin density distribution of the oxidized P680 will be found.

Acknowledgements

A.K. is indebted to Hyogo Science and Technology Association for the financial support of this work.

References

[1] R.J. Debus, Biochim. Biophys. Acta 1102 (1992) 269–352.
[2] A.-F. Miller, G.W. Brudvig, Biochim. Biophys. Acta 1056 (1991) 1–18.
[3] D.R. Ort, C.F. Yocum (Ed.), Oxygenic Photosynthesis: The Light Reactions, Kluwer Academic Publisher, New York, 1996.
[4] A.W. Rutherford, J.L. Zimmerman, Biochim. Biophys. Acta 767 (1984) 168–175.
[5] V.V. Klimov, E. Dolan, B. Ke, Proc. Natl. Acad. Sci. USA 77 (1980) 7227–7231.
[6] F. MacMillan, F. Lendzian, G. Renger, W. Lubitz, Biochemistry 34 (1995) 8144–8156.
[7] Y. Sanakis, V. Perrouleas, B.A. Diner, Biochemistry 33 (1994) 9922.
[8] A.V. Astashkin, A. Kawamori, Y. Kodera, S. Kuroiwa, K. Akabori, J. Chem. Phys. 102 (1995) 5583–5586.
[9] Y. Deligiawakis, C. Jegerschöld, A.W. Rutherford, Chem. Phys. Lett. 270 (1997) 564–572.
[10] G. Renger, J. Kurreck, E. Haag, F. Reifarth, A. Bergmann, F. Parak, in: A.X. Trautwein (Ed.), Bioinorganic Chemistry, VCH, Weinheim, 1997, pp. 160–177.
[11] H. Hara, S.A. Dzuba, A. Kawamori, K. Akabori, T. Tomo, K. Satoh, M. Iwaki, S. Itoh, Biochemistry 1322 (1997) 77.
[12] S.G. Zech, J. Kurreck, H.J. Eckert, G. Renger, W. Lubitz, R. Bittl, FEBS Lett. 414 (1997) 454–456.
[13] V.V. Kurshev, A.M. Raitsimring, Yu.D. Tsvetkov, J. Magn. Reson. 81 (1989) 441.
[14] V.V. Kurshev, A.M. Raitsimring, T. Ichikawa, J. Phys. Chem. 95 (1991) 3564–3568.
[15] A.V. Astashkin, Y. Kodera, A. Kawamori, Biochim. Biophys. Acta 1187 (1994) 89–93.
[16] Y. Kodera, H. Hara, A.V. Astashkin, A. Kawamori, T.-A. Ono, Biochim. Biophys. Acta 1232 (1995) 43–51.
[17] H. Hara, A. Kawamori, A.V. Astashkin, T.-A. Ono, Biochim. Biophys. Acta 1276 (1996) 140–146.
[18] K. Shigemori, H. Hara, A. Kawamori, K. Akabori, Biochem. Biophys. Acta 1363 (1998) 187–198.
[19] A.V. Astashkin, H. Hara, A. Kawamori, J. Chem. Phys. 108 (1998) 3805–3812.
[20] A.W. Rutherford, Biochim. Biophys. Acta 807 (1985) 189–201.
[21] P.J. O'Malley, G.T. Babcock, R.C. Prince, Biochim. Biophys. Acta 766 (1984) 283–288.
[22] C.W. Hoganson, G.T. Babcock, Biochemistry 31 (1992) 11874–11880.
[23] H. Mino, J.-I. Satoh, A. Kawamori, K. Toriyama, J.-L. Zimmermann, Biochim. Biophys. Acta 1144 (1993) 426–433.
[24] H. Mino, A. Kawamori, Biochim. Biophys. Acta 1185 (1994) 213–220.
[25] T. Kuwabara, N. Murata, Plant Cell Physiol. 23 (1982) 533–539.
[26] D.F. Ghanotakis, D.M. Demetriou, C.F. Yocum, Biochim. Biophys. Acta 891 (1987) 15–21.
[27] D. Koulougliotis, X.-S. Tang, B.A. Diner, G.W. Brudvig, Biochemistry 34 (1995) 2850–2856.
[28] A.D. Milov, K.M. Salikov, M.D. Shirov, Fiz. Tverd. Tela (Leningrad) 23 (1981) 975-982 (in Russian).
[29] A.D. Milov, A.B. Ponomarev, Yu.D. Tsvetkov, Chem. Phys. Lett. 110 (1984) 67–72.
[30] K.-H. Ree, E.P. Morris, J. Barber, W. Kühlbrandt, Nature 396 (1998) 283–286.
[31] J. Barber, Biochim. Biophys. Acta 1365 (1998) 269–277.
[32] J. Barber, Trends Biochem. Sci. 12 (1987) 123–124.
[33] H. Michel, J. Deisenhofer, Biochemistry 27 (1988) 1–7.
[34] J.P. Allen, G. Feher, T.O. Yeates, H. Komiya, D.C. Rees, Proc. Natl. Acad. Sci. USA 85 (1988) 8487–8491.
[35] T. Yoshii, H. Hara, A. Kawamori, K. Akabori, M. Iwaki, S. Itoh, Appl. Magn. Reson., in press.
[36] S.E.J. Rigby, H.H.A. Nugent, P.J. O'Malley, Biochemistry 33 (1994) 10043–10050.